6th International Meeting
on
Wind Turbine Noise
Glasgow 20-23 April 2015

Numerical Investigation of the Aeroacoustics of Small Vertical Axis Wind Turbines

Johannes Weber, Institute of Process Machinery and Systems Engineering, Cauerstraße 4, 91058 Erlangen Germany. wb@ipat.uni-erlangen.de

Stefan Becker, Institute of Process Machinery and Systems Engineering, Cauerstraße 4, 91058 Erlangen Germany. sb@ipat.uni-erlangen.de
Christoph Scheit, Institute of Process Machinery and Systems Engineering Cauerstraße 4, 91058 Erlangen Germany.
Andreas Hüppe, Vienna University of Technology, Wiedner Hauptstraße 8, 1040 Vienna, Austria. andreas.hueppe@tuwien.ac.at
Manfred Kaltenbacher, Vienna University of Technology, Wiedner Hauptstraße 8, 1040 Vienna, Austria. Manfred.kaltenbacher@tuwien.ac.at

Summary

Understanding the physical mechanisms of noise generation of wind turbines is an important factor to design turbines at a low-noise level and therefore for increasing social acceptance. Beside the horizontal wind turbines, small wind turbines are considered as a possible solution for harvesting wind energy especially at small scales in urban areas. CFD programs have been used successfully for the aerodynamic design of vertical axis wind turbines. For the acoustic design, numerical simulations studies on noise emission are hardly available today. To investigate the aeroacoustics of small vertical axis wind turbines, a hybrid approach is chosen where first a CFD simulation is performed and the acoustics are calculated in a second step. Two different methods are compared for the acoustic simulation: an integral method described by Ffowcs-Williams-Hawkings (FW-H) function and a Finite Element Method, which is based on the analogy of Lighthill. Using an in-house solver for the FW-H calculation, the flow quantities are interpolated to an integration surface placed around the vertical axis wind turbine and are exported from the CFD calculation. From this integration surface, Green's function is used to calculate the acoustically relevant parameters in the far field. In case of the Lighthill's analogy, the sound sources are calculated in the form of the divergence of the Lighthill tensor from the velocity and the density on the CFD grid and are exported. These acoustic sources are interpolated to an acoustic grid. Following that, the propagation of sound is calculated in the far field.The experimental measurements took place in an anechoic wind tunnel. These results are found to be in very good agreement with measurements.

1. Introduction

Wind energy is one of the most important renewable energy source, which arises in more installations in the vicinity of urban areas. Beside the visual impact caused by wind turbines, a low noise design is essential for public acceptance. Noise is defined as a subjective perceiption of sound waves by the human ear, which is unwanted. Therefore, it is important to reduce the sound emission to avoid annoyance of people, which are living close to wind turbines [1]. Beside the large horizontal wind turbines, which are the most common configuration for harvesting wind energy, the interest in small wind turbines are grown in the last years because of the possible future demand for a decentralised and sustainable power generation in rural environments and

cities. Due to the turbulent wind environments in cities, vertical axis wind turbines (VAWT) are more focused by research and development. VAWTs offer some advantages in comparison to their horizontal counterparts, which can be useful especially in complex wind situations in cities. One of the most important advantage is the insensitivity of fast changing wind directions, which avoids the need of a yaw system. Further benefits are the better efficiency in turbulent wind streams, lower sound emissions and the better aesthetic appearance. In order to design a high performance vertical axis wind turbine, it is inalienable to get the physical understanding of the flow physics and the acoustics, which are very complex [2], [3].

In this study, a complementary approach consisting of experimental measurements, computational fluid dynamics simulations and aeroacoustics simulations were performed. The subject of interest is a straightbladed H-darrieus turbine. The aeroacoustics simulations are performed by applying two different in-house codes. The first code, which is called CFS++, is based on Lighthill's analogy [4], [5], [6]. It is implemented in a finite-element solver. With the help of this code, it is possible to understand the development and propagation of acoustic source terms.

The second one is called SPySI (sound prediction by surface integration), which is predicated on the porous Ffowcs Williams-Hawkings method [7].

In recent years, experimental and numerical investigations, which are mostly focused on the aerodynamic behaviour, were performed in the field of VAWTs, e.g., by Mohamed, who investigated the aerodynamic performance of the H-Darrieus turbine with different airfoil shapes [8]. Simão Ferreira placed the focus on the research of dynamic stall [9]. Mertens investigated the performance of an H-Darrieus in the skewed flow on a roof in urband areas [10]. Marnett studied a multiobjective numerical design of vertical axis wind turbine components in his PhD thesis [11]. Beside of the aerodynamic investigations of VAWTs, just a few publications on noise emission are available today. Iida investigated numerically the aerodynamic sound of a VAWT by using discrete vortex methods. This paper pointed out that a HAWT generates more noise as a VAWT with the same power coefficient at normal operating speed [12]. In 2013, Pearson has performed an investigation of the noise sources on a VAWT using an acoustic array. He stated that at low frequencies the harmonic components are dominating the spectrum. At low tip-speed ratio the harmonics were much stronger in comparison to those at higher tip-speed ratio. Therefore, Pearson suggested that at low tip-speed ratio the unsteady blade loading is much higher due to the dynamic stall effect [13]. Mohamed investigated numerically the noise emission of a Darrieus turbine using a Ffowcs-Williams and Hawkings method. This paper shows a parameter study, in which the blade shape, tip-speed ratio and solidity effects were varied. He came to the conclusion, that the higher tip-speed ratio and higher solidity rotors generate more noise than normal turbines [14].

2. Experimental setup

The experimental measurements took place in an anechoic wind tunnel at the University of Erlangen-Nürnberg, which is schematically depicted in figure 1. The aeroacoustic wind tunnel is characterized of the closed return with an open test section. This section is located in an anechoic chamber, so that free field acoustic measurements without any reflections from the walls can be performed. The absorption coefficient of this chamber has a factor of 0.9 for a frequency of 300 Hz. In order to assure a low noise level in the test section, the wind tunnel possess silencers to damp out fan noise. The nozzle of the wind tunnel has a cross-section area of 0.25 m x 0.33 m and achieves a maximum wind speed of 35 m/s. A low turbulence level of 0.15% in the wind tunnel is accomplished because of several turbulence grids and a honeycomb. The subject of these investigations is a generic model scale rotor of a 3-bladed H-Darrieus turbine as illustrated in fig. 1. The airfoil profile NACA0018 was chosen because of its good aerodynamic performance for VAWTs as described in literature [15]. Due to the small wind tunnel working section, a model of 0.2 m diameter and height is used. The chord length c of the model was chosen as 0.05 m.

In order to characterize the blade aerodynamics and the relevant noise mechanisms the Reynolds number will be referred to chord length c and the angular velocity $\omega = 2\pi nr$. In case of the validation test case ($v = 25\, m/s$), which we present in the following sections, the Reynolds number reaches a value of $Re_c = 121365$ at a rotating speed of 3500 rpm.

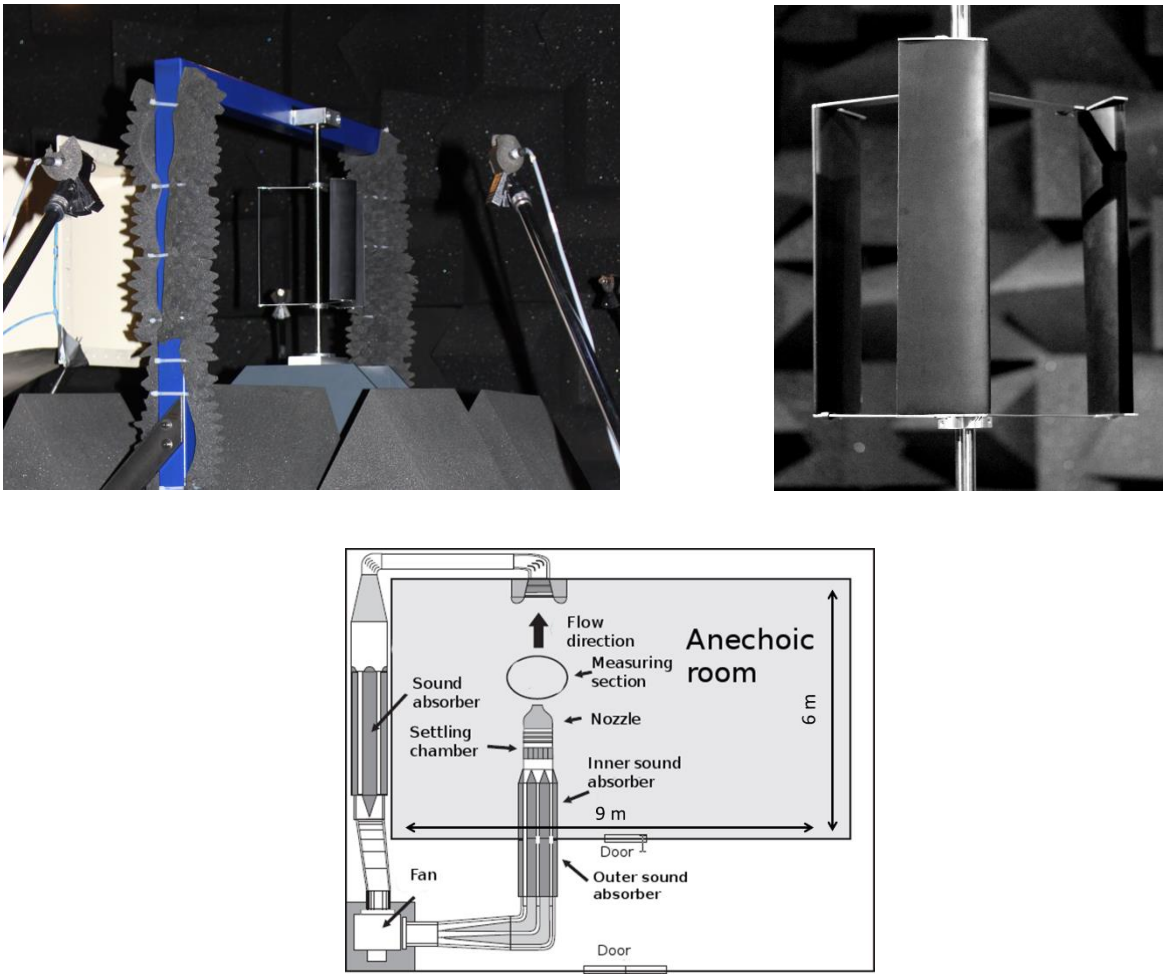

Fig. 1: Experimental set-up (top left), the model scale rotor (top right) and the anechoic wind tunnel (bottom)

One of the most important quantities for the aerodynamic performance is the rotor solidity, which is defined as $\sigma = Nc/(2\mathrm{r})$ where N represents the number of blades, c the chord length of the blade and r is the radius. It describes how much of the horizontal turbine projection area $A = 2hr$ is covered by the airfoils which in turn affects the amount of deflection of the incoming flow [11]. In order to measure the acoustic pressure, four ½-inch free-field microphones (Bruel & Kjaer type 4189) were positioned in a half circle in equal angles of 45 degrees at a distance of l = 1 m. The microphones have a linear frequency response characteristic. Furthermore, the frequency spectrum ranges between 6.3 Hz and 20 kHz and the dynamic range is from 14.6 dB to 146 dB. These were connected with a Nexus amplifier type 2690-A-0S4 of Bruel & Kjaer. In order to convert the signal, a National Instrument PXIe-4492 A/D converter was used. The height of the microphones was chosen as h = 1.9 m, which is the middle of the rotor height. The distance between the outlet of the nozzle and the center of the model is s = 0.33 m. The rotor speed of the model can be adjusted by the servomotor Siemens Simotics S 1Fk7. In order to measure the torque of the model scale, a torque sensor with a measuring range of 1 Nm was used. By measuring the pressure drop along the nozzle and applying Bernoulli's formula the desired wind speed is adjusted. A schematic drawing of the experimental set-up is depicted in figure 2.

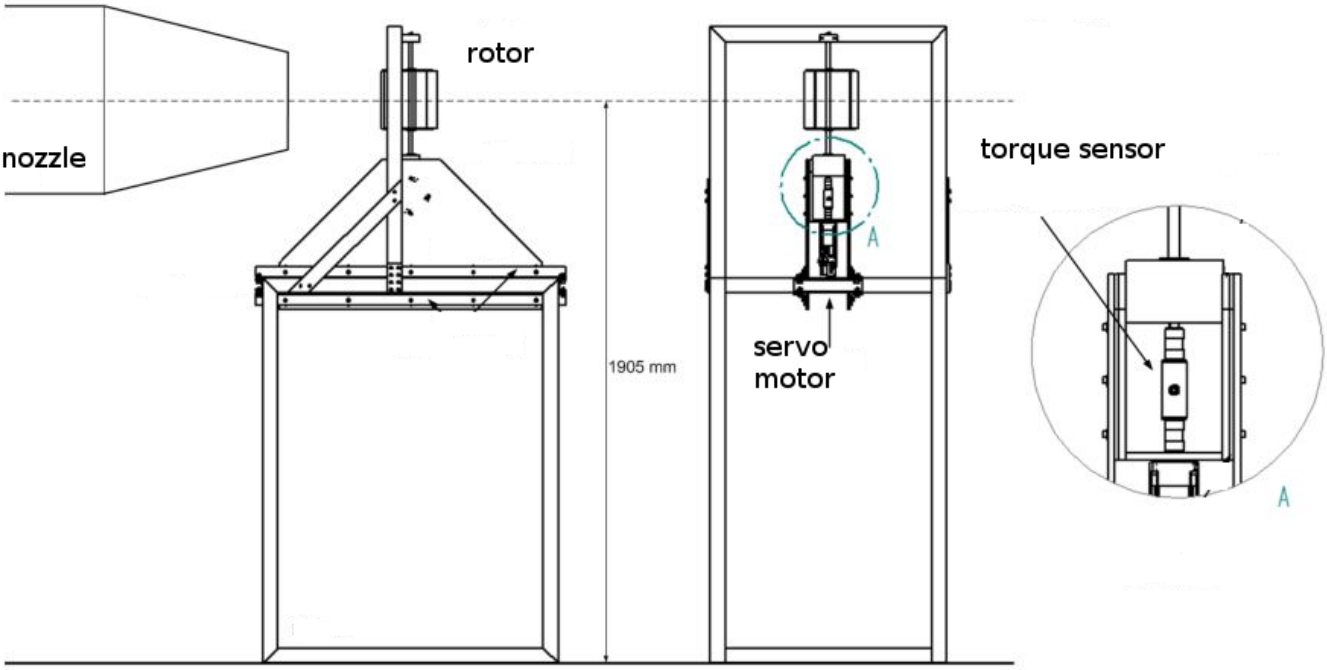

Fig. 2: Schematic drawing of the experimental set-up with torque sensor and servomotor

3.0 Computational methods

3.1 Aerodynamic simulation

In order to understand the physics of flow, the CFD simulation of the straightbladed H-Darrieus wind turbine experimental measurements are validated with the help of the CFD simulations. Therefore, the design of an H-Darrieus wind turbine as illustrated in fig. 1 is used for the turbulent flow field computation by the finite-volume method solver ANSYS-CFX 15.0 [16]. Figure 3 shows the circumferential computational fluid domain composed of a rotating and a stationary region, which are connected by a transient rotor stator interface. The inlet of the fluid domain is located on the left half of the outer circle and the inlet boundary condition was given by v = 25 m/s wind speed. At the outlet, an opening boundary condition was defined at relative pressure 0 Pa in order to allow backflow that means vortices are permitted to pass the outlet boundary. This results in in- and outflow at the same time. The rotational speed of the airfoils was set to $n = 3500$ rpm. At this operating point a tip-speed ratio $\lambda = 2\pi nr/v$ of 1.44 is achieved, which is the optimum tip-speed ratio of this configuration in the experimental measurements. Here, the turbulence model URANS-SST (Shear Stress Tansport) was applied. A hexahedral mesh consisting of 13 Mio cells, of which 10.3 Mio cells are located in the rotating region, was generated in ANSYS ICEM [16]. Due to the rotational symmetry of the rotor, one third of the turbine was meshed and rotated to the full 360 degree geometry. Conforming, periodic interfaces were placed at the outer edges of the grid in order to make sure that every node matches after the rotation of the mesh. Ensuring that the boundary layers on the blades and on the shaft are adequately resolved, the mesh is strongly refined to obtain a normalized distance of the wall nearest grid cell of $y^+ < 1$. In order to affirm mesh independency, a grid study was performed prior to this work.

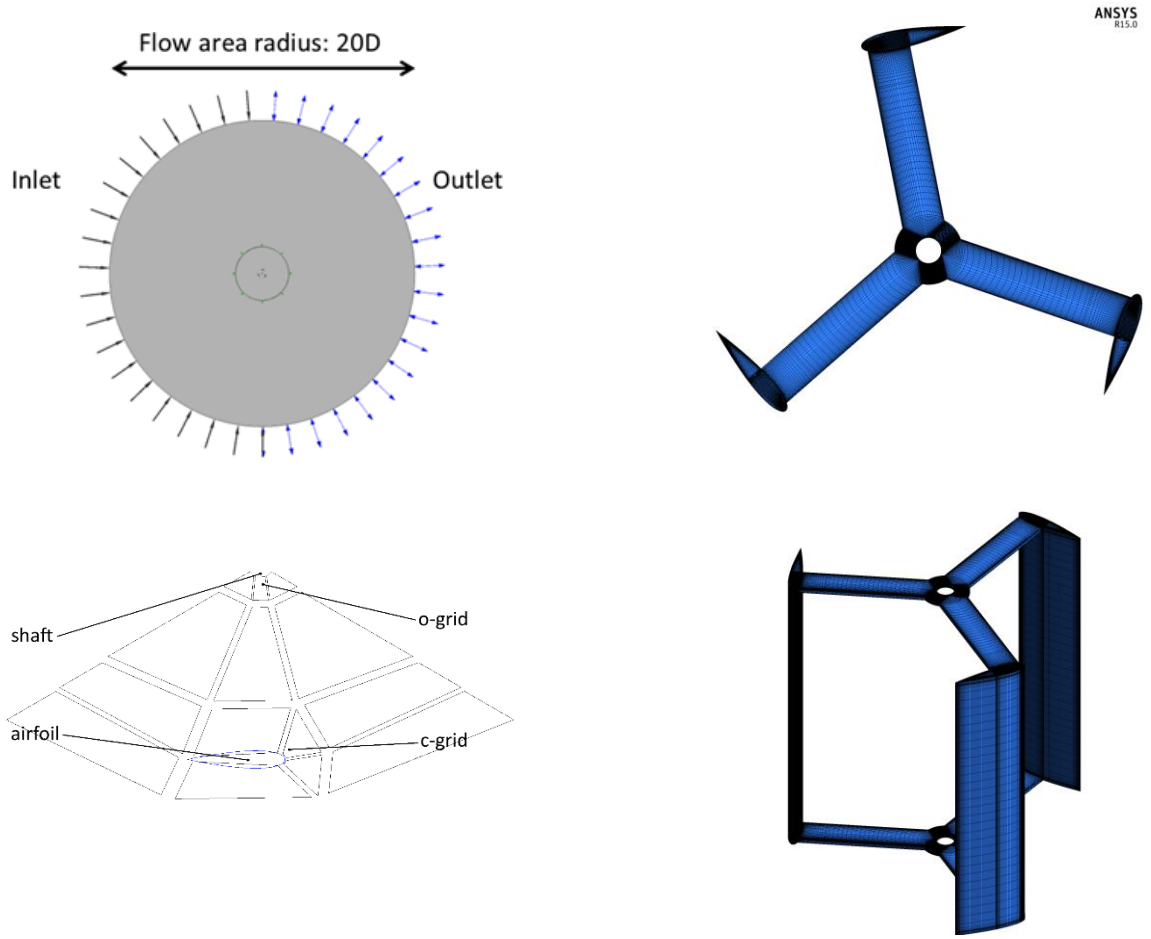

Fig. 3: Computational domain of the CFD simulation (top left) and illustration of the block strategy (bottom left), the mesh topology of the struts (top right) and isometric view on gird topology at the airfoils (bottom)

3.2 Aeroacoustic formulation

In order to calculate the sound pressure spectra radiated by the H-Darrieus, the acoustic analogies established by Lighthill [17], [18] on one hand and Ffowcs Williams and Hawkings [19] on the other hand are used and will be presented in the following.
The computation of flow-induced noise according to Lighhill's analogy starts with his famous inhomogeneous wave equation for the sound pressure p'

$$\frac{1}{c_0^2}\frac{\partial^2 p'}{\partial t^2} - \frac{\partial p'}{\partial x_i^2} = \frac{\partial^2 T_{ij}}{\partial x_i \partial x_j} \tag{1}$$

The left hand side is equivalent to the homogenous wave equation. The right hand side which is the Lighthill tensor T_{ij} is the source term of the complete inhomogeneous wave equation. It was derived by Lighthill directly from the conservation of mass and momentum.

$$T_{ij} = P_{ij} + \rho u_i u_j - c_0^2 \delta_{ij} \rho' = \rho u_i u_j + (p' - c_0^2 \rho')\delta_{ij} - \tau_{ij}, \tag{2}$$

which consists of non-linear convective forces $\rho u_i u_j$, deviations in the speed of sound c_0, $(p' - c_0^2 \rho')$, viscous forces τ_{ij}, and the Kronecker delta δ_{ij}.
A further simplification of the Lighthill tensor can be accomplished in case of an isotropic flow at low Mach numbers. In this case, viscous effects $\tau_{ij}$are negligible. Also, the term $(p' - c_0^2 \rho')$ is only relevant for anisotropic media and can be considered to be very small in air. Only the non-linear convective effects $\rho u_i u_j$ remain as sound sources which results in

$$T_{ij} \approx \rho_0 u_i u_j \tag{3}$$

Since we solve directly the Lighthill's inhomgeneous wave equation by the FE method, we implicitely take all acoustic source mechanism into account. To obtain a formulation suitable for finite element-methods, a weak formulation of Lighthill's inhomogeneous wave equation is developed. For this purpose, eq. (1) is multiplied by an appropriate element shape function w, integrated over the computational domain Ω and Stokes' integral theorem is applied.

$$\int_{\Omega} \frac{1}{c_0^2}\frac{\partial^2 p'}{\delta t^2}\mathrm{w}\mathrm{d}\Omega + \int_{\Omega} \frac{\partial w}{\partial x_i}\frac{\partial p'}{\partial x_i}\mathrm{d}\Omega - \int_{\Gamma} \frac{\partial p'}{\partial n} w\,\mathrm{d}\Gamma = -\int_{\Omega} \frac{\partial w}{\partial x_i}\frac{\partial T_{ij}}{\partial x_j}\mathrm{d}\Omega \tag{4}$$

For details concerning the FE formulation, we refer to [4].

As a second approach, we have chosen the porous Ffowcs Williams-Hawkings method, which is based on an integral solution of eq. (1).

$$\begin{aligned} 4\pi\{p'H(f)\} = {} & \frac{\partial^2}{\partial x_i \partial x_j}\int_{R^3}\left[\frac{T_{ij}H(f)}{r|M_r-1|}\right]_{\tau_e}\mathrm{d}^3\eta_j + \frac{\partial}{\partial t}\int_S \left[\frac{[\rho(u_i - v_i\ ) + \rho_0 v_i]n_i}{r|M_r-1|}\right]_{\tau_e}\mathrm{d}S(\eta_j) \\ & + \frac{\partial}{\partial x_j}\int_S \left[\frac{[\rho u_j(u_i - v_i\ ) + P_{ij}]n_i}{r|M_r-1|}\right]_{\tau_e}\mathrm{d}S(\eta_j) \end{aligned} \tag{6}$$

The first term of the equation at the right hand side represents the quadrupole sources, which are generated by the turbulent wakes by the wind turbine. The variable $H(f)$ corresponds to the Heaviside function, M_r equates to the radial Mach number and T_{ij} is the Lighthill tensor. The second term is called thickness noise and is caused by the displacement of the air by the rotor blades. The size u_i describes the fluid velocity and v_i characterizes the velocity of the surface. The last term is named loading noise and corresponds to the sound which is generated by the acceleration of the force distribution on the air around the rotor blade. This term includes the compressive stress tensor P_{ij}.

$$P_{ij} = (p - p_0)\delta_{ij} + \tau_{ij}$$

For calculation of radiation into free field, the FW-H can be solved with the free-space Green's function [20],

$$G(x,t) = \frac{\delta(t - |x_i - y_i| - \tau/c_0)}{4\pi|x_i - y_i|}, \tag{7}$$

where c_0 represents the ambient speed of sound and τ is the retarded time.

3.3 Aeroacoustic Simulation

In order to apply SPySI for the FW-H calculation, the three velocity components, the pressure and the density are interpolated onto the integration surface placed around the acoustic sources which are generated by the wind turbine (see Fig. 4). The flow variables of interest are exported from the CFD calculation at every time step. In this study, the integration surface is placed in a distance of 0.4 m from the center. It should be positioned near as possible to the acoustic sources in order to prevent the influence of numerical damping. If the surface is located too close to the flow field, there is a risk that not only acoustical pressure fluctuations are included, but also hydrodynamic pressure, which is unwanted.

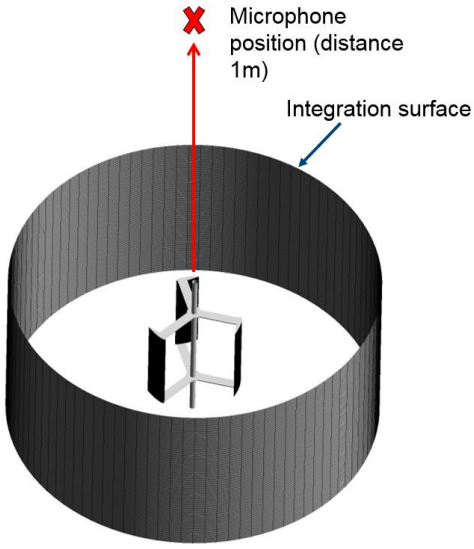

Fig. 4: Integration surface on which the flow variables are interpolated

4.0 Results and discussion

4.1 Experimental results

In order to get the value of the optimum tip-speed ratio, experimental measurements were performed prior to the CFD simulation. Different rotating speeds from 1500 rpm to a maximum of 4000 rpm were adjusted at a constant wind speed of 25 m/s. The difference of the torque of the torque sensor and the servo motor was measured to calculate the efficiency cp of the rotor. In fig. 5 the trend of the cp-λ curve is illustrated. The maximum cp has a value of 0.22 at a tip-speed ratio of 1.44.

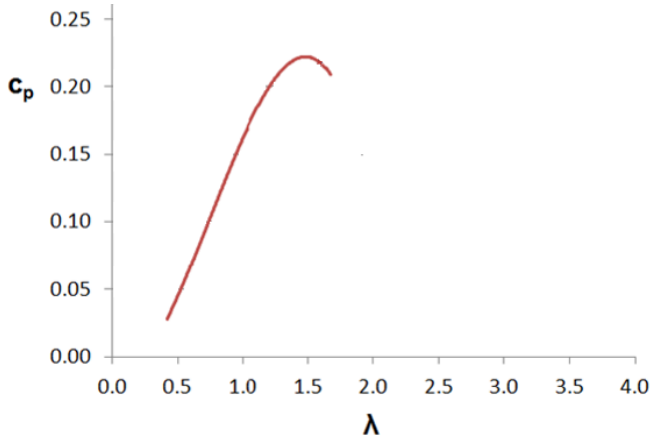

Fig. 5: Experimental measurement of the cp-λ- curve

The sound pressure level spectrum is depicted in fig. 6. The first major peak belongs to the blade passing frequency of 175 Hz. Higher Harmonics can be detected up to the 13th one. Between these harmonics small peaks can be seen which refer to the noise of the bearings. Furthermore, broadband noise appears at around 2000 Hz and becomes dominant at frequencies above 3000 Hz. The tonal peak at the frequency of 8000 Hz refers to the generator noise.

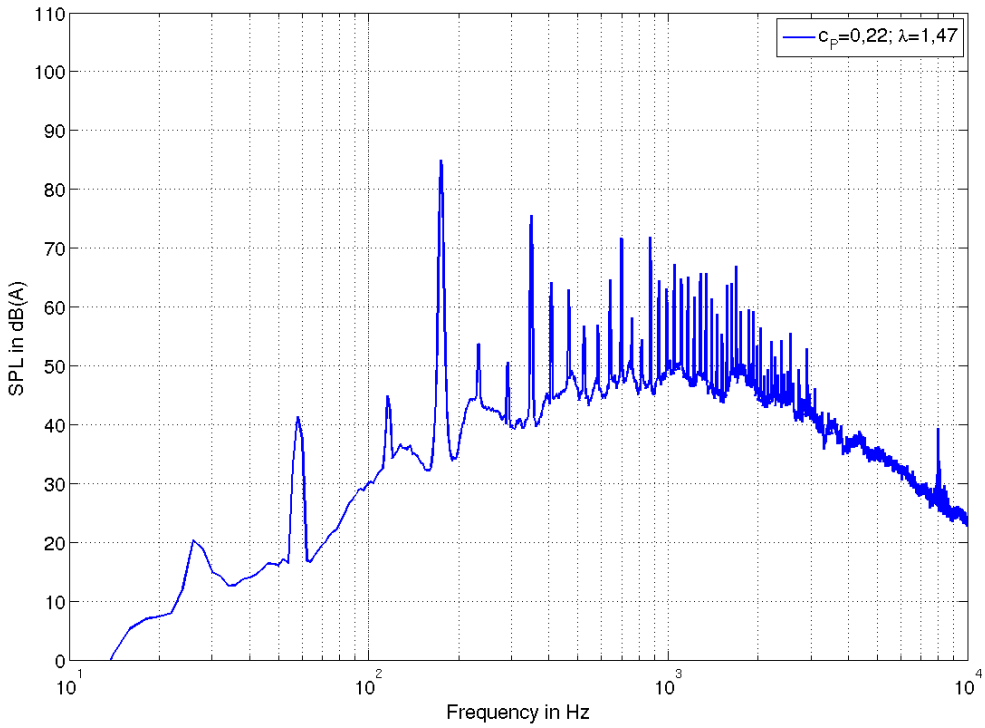

Fig. 6: Experimental data at rotating speed of 3500 rpm and wind speed of v = 25 m/s (Reynolds number = 121365)

4.2 Simulation results

In the following, the CFD results will be presented. To illustrate the transient flow field the temporal development of the flow of the rotor is presented in fig. 7. Due to the rotational symmetry, a whole revolution can be depicted by 120°. In order to visualize the vortex structures of the flow, the vorticity in the stationary frame at a value of 2200 1/s is used. In this illustration, the wind is arriving from the left side and the rotation direction of the wind turbine is counter clockwise. Referring to Dixon [22] the VAWT wake is epicycloidal, if it is viewed along its axis of rotation. Due to the turbines movement it will cut its own wake during normal operation. That leads to strong blade vortex interaction. Highly turbulent structures can be seen at the blade tip of the turbine. The tip vortices move quickly inwards after being released and are intersected by downwind blade pass. Furthermore, a large vortex structure is separating from the trailing edge, which has an impact of the following blade.
In this simulation the shaft itself is a source of vortex generation and separation.

0°

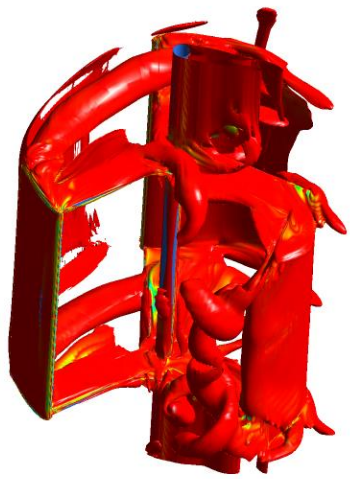

40°

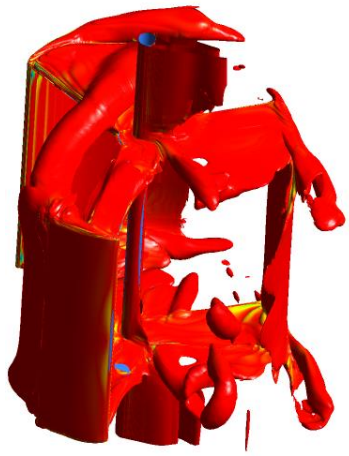

80°

120°

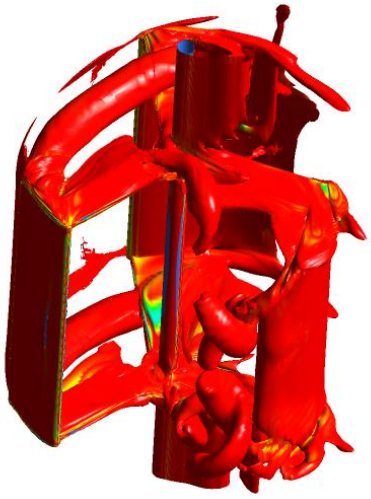

Fig. 7: Temporal development of the vorticity in stationary frame at 2200 1/s

Beside the CFD results, the acoustic results will be presented in the following. This includes the localization of the acoustic source terms on the one hand and the validation of the computed sound radiation by applying the FW-H code with measurements on the other hand.

According to Pearson [23] the different noise mechanisms on his model VAWT was Dynamic Stall Noise, Laminar Boundary Layer Tonal Noise, Trailing Edge Noise [21] and Blade-Wake Interaction Noise.

If one consider the acoustic source terms in fig. 8, which are calculated by the FE-Simulation, large acoustic sources can be detected on both ends of the airfoil, which are moving instream and will be intersected by the strut and the blade of the downstream airfoil.
Furthermore, the vortex separation at the trailing edge will also have an impact on the overall acoustic. In general, there is a high interaction between the different vortices and the blades.

0°

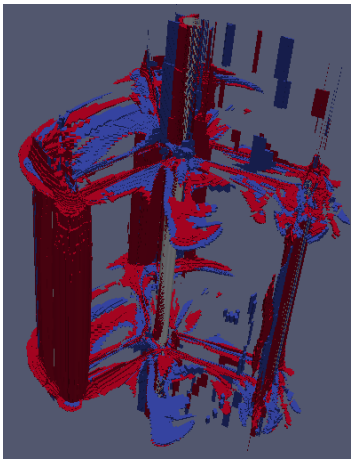

40°

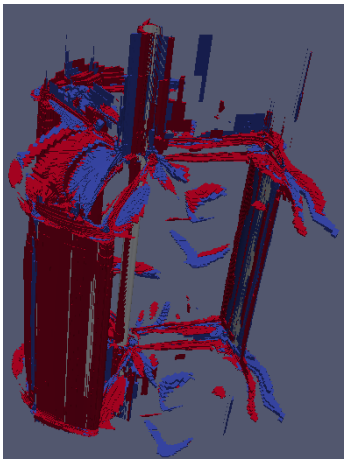

80°

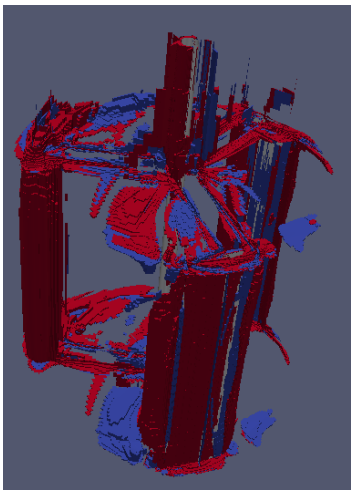

120°

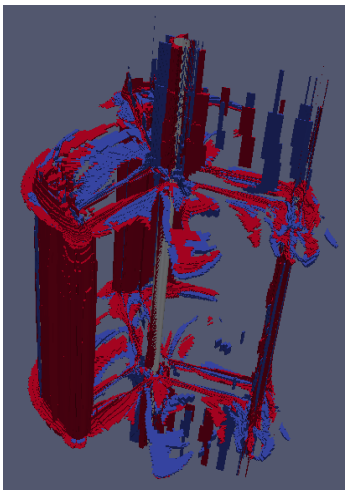

Fig. 8: Temporal development of the acoustic source terms calculated by the theory of Lighthill

Figures 9 shows the comparison between the measurement and the FW-H simulation. The acoustic pressure of the straightbladed H-Darrieus turbine are computed with the in-house code SPySI. To calculate the sound pressure spectrum of the simulation and measurment, a Fast Fourier Transformation is done of the simulated time with the length of 0.41 s, which corresponds to 24 rotations of the wind turbine. A rectangular window with an overlap of 50 percent was used for the FFT. The sound pressure spectrum of simulation and measurement indicates well to very good agreement dependent on the frequency. The height of the amplitude of the BPF at 175 Hz will be captured very well. 10 higher harmonics of the BPF can be resolved by the simulation. In the region of 1000 Hz, the FW-H inhouse-code underestimate the noise level of the measurement by a small margin. At a frequency of 2000 Hz random noise is dominating in the simulation. This is caused by the URANS-Turbulence model, which can only resolve the larger vortices. The smaller vortices, which are responsible for noise generation in the high frequency range could not be resolved. In order to resolve the broadband noise accurately

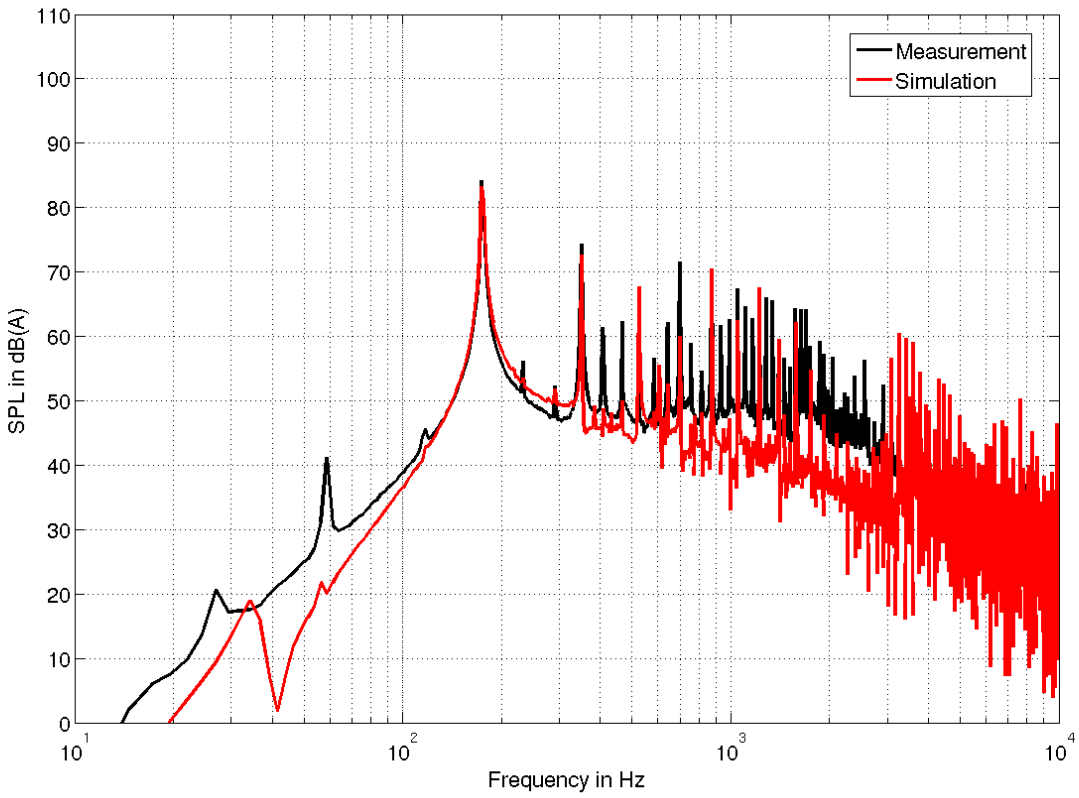

Fig. 9: Sound pressure level spectra of FW-H Simulation (red) and the exerpimental measurement (black)

5.0 Conclusion

CFD and CAA simulations were performed of the straightbladed Darrieus turbine. In this study, a URANS simulation was performed in order to compute the flow field. Calculating the sound propagation of the turbine, a FW-H inhouse-code was used. The acoustic computation indicates in case of the tonal components very good agreement. In case of the broadband noise at higher frequencies, the simulation underestimates the noise level, because of the chosen turbulence model URANS. In order to get a better agreement in this frequency range, a Scale Adaptive Simulation or Large Eddy Simulations has to be performed in future. The acoustic source terms, which are calculated by the theory of Lighthill give an impression about the production of the sound at this operating point. In further investigations frequency filtering of the acoustic source terms should be applied in order to investigate the contribution of the different noise mechanisms to the overall sound emission.

Acknowledgements

This work is supported by the Bavarian research project E|Home-Center [24], which is funded by the Bavarian government.

References

[1] Manwell, J.F. (2009) *Wind Energy Explained – Theory, Design and Application 2nd Edition,* John Wiley & Sons Ltd

[2] Paraschivoiu, I. (2002) *Wind Turbine design – With Emphasis on Darrieus Concept* Presses Internationales Polytechnique

[3] Milborrow, D. (1995) *Vertical axis wind turbines* WindStats Newsletter 8, pp. 5-8

[4] M. Kaltenbacher, M. Escobar, I. Ali and S. Becker (2010), *Numerical Simulation of Flow-Induced Noise Using LES/SAS and Lighthill's Acoustics Analogy*, International Journal for Numerical Methods in Fluids, Vol. 63(9), pp. 1103–1122

[5] Flemisch, B., Kaltenbacher, M., and Wohlmuth, B. I (2006) *Elasto-acoustic and acoustic-acoustic coupling on nonmatching grids,* Int. J. Numerical Methods in Engineering, Vol. 67, No. 13, pp. 1791–1810.

[6] Escobar, M. (2007) *Finite Element Simulation of Flow-Induced Noise using Lighthill's Acoustic Analogy* PhD thesis, University of Erlangen-Nuremberg

[7] Scheit, C., Karic, B. and Becker, S. (2011) *Effect of blade wrap angle on efficiency and noise of small radial fan impellers – A computational and experimental study* Journal of Sound and Vibration, No. 331, No. 5, pp. 996-1010

[8] Mohamed, M.H. (2012) *Performance investigation of H-Rotor Darrieus Turbine with the new airfoil shapes,* Energy, Vol. 47, pp. 522-530

[9] Ferreira, C.J. (2009) *The near wake of the VAWT -2D and 3D views of the VAWT aerodynamics* PhD thesis, TU Delft

[10] Mertens, S. (2006) *Wind Energy in the Built Environment* PhD thesis, TU Delft

[11] Marnett, M. (2012) *Multiobjective Numerical Design of Vertical Axis Wind Turbine Components* PhD thesis, RWTH Aachen

[12] Iida, A., Mizuno, A. and Fukodome, K. (2004) *Numerical Simulation of Aerodynamic Noise radiation from Vertical Axis Wind Turbines* Technical Report, Kogakuin University Department of Mechanical Engineering

[13] Pearson, C. and Graham, W. (2013) *Investigation of the noise sources on a vertical axis wind turbine using an acoustic array* 19th AIAA/CEAS Aeroacoustics Conference, Berlin

[14] Mohamed, M.H. (2013) *Aeroacoustics noise evaluation of H-rotor Darrieus wind turbines* Energy, Vol. 65, pp. 596-604

[15] Timmer, W.A. (2008) *Two-dimensional low-Reynolds number wind tunnel results for airfoil NACA0018,* Wind Engineering, Vol. 32, pp. 525-537

[16] ANSYS, ANSYS, fourteenth ed. www.ansys.com

[17] Lighthill, J.M. (1952) *On Sound Generated Aerodynamically I. General Theory,* Proceedings of the Royal Society, Vol. 211, No. 1107, pp. 564–587.

[18] Lighthill, J.M. (1954) *On Sound Generated Aerodynamically II. Turbulence as a Source of Sound,* Proceedings of the Royal Society, pp. 1–32.
[19] Ffowcs Williams, J. E. and Hawkings, D. L. (1969) *Sound Generation by Turbulence and Surfaces in Arbitrary Motion* Philosophical Transactions of the Royal Society, Vol. 264, No. 1151, pp. 321–342.
[20] Ehrenfried, K. (2004) *Strömungsakustik (Aeroacoustics*) Mensch & Buch Verlag, pp. 145-159
[21] Brooks, T.F., Pope, D.S., Marcolini, A. (1989) *Airfoil Self-Noise and Prediction,* NASA Reference Publication 1218
[22] Dixon, K., Ferreria, C.S., Hofemann, C. (2008) A 3D Unsteady Panel Method for Vertical Axis Wind Turbines, EWEC, Brussel
[23] Pearson, C. (2014) *Vertical Axis Wind Turbine Acoustics* Cambridge University Engineering Department
[24] E|Home-Center, www.ehome-center.de